The Astrophysical Journal, 613:1133–1142, 2004 October 1

MASSIVE BLACK HOLES IN STAR CLUSTERS. I. EQUAL-MASS CLUSTERS

Holger Baumgardt,[1] Junichiro Makino,[2] and Toshikazu Ebisuzaki[1]
Received 2004 March 15; accepted 2004 June 4

ABSTRACT

In this paper we report results of collisional N-body simulations of the dynamical evolution of equal-mass star clusters containing a massive central black hole. Each cluster is composed of between 5000 and 180,000 stars together with a central black hole that contains between 0.2% and 10% of the total cluster mass. We find that for large enough black hole masses, the central density follows a power-law distribution with slope $\rho \sim r^{-1.75}$ inside the radius of influence of the black hole, in agreement with predictions from earlier Fokker-Planck and Monte Carlo models. The tidal disruption rate of stars is within a factor of 2 of that derived in previous studies. It seems impossible to grow an intermediate-mass black hole (IMBH) from an $M \leq 100\ M_{\odot}$ progenitor in a globular cluster by the tidal disruption of stars, although $M = 10^3\ M_{\odot}$ IMBHs can double their mass within a Hubble time in dense globular clusters. The same is true for the supermassive black hole at the center of the Milky Way. Black holes in star clusters will feed mainly on stars tightly bound to them, and the repopulation of these stars causes the clusters to expand, reversing core collapse without the need for dynamically active binaries. Close encounters of stars in the central cusp also lead to an increased mass-loss rate in the form of high-velocity stars escaping from the cluster. A companion paper will extend these results to the multimass case.

Subject headings: black hole physics — globular clusters: general — methods: n-body simulations — stellar dynamics

1. INTRODUCTION

Theoretical studies of the dynamics of massive black holes (BHs) in dense stellar systems started in the 1960s to explain the central activity and luminosities of quasars. Since then, the dynamics of a massive body in the center of a stellar system has been the focus of a large number of theoretical studies, starting with classic papers by Peebles (1972), Bahcall & Wolf (1976, 1977), Frank & Rees (1976), and Cohn & Kulsrud (1978).

The problem is of great importance to astrophysics, since the centers of the Milky Way and other nearby galaxies contain BHs of 10^6–$10^9\ M_{\odot}$ (Kormendy & Gebhardt 2001). In addition, smaller sized BHs of a few thousand solar masses might exist in globular clusters (Gerssen et al. 2002, 2003; Gebhardt et al. 2002; Portegies Zwart et al. 2004), although the evidence for these is still controversial (Baumgardt et al. 2003a, 2003b). A massive BH in a galactic nucleus or a star cluster is a potential source of gravitational radiation owing to its high mass and the fact that it will frequently undergo close encounters with other stars and BHs if the density of the surrounding system of stars is high enough. It would therefore be a prime target for the forthcoming generation of ground- and space-based gravitational wave detectors.

Intermediate-mass BHs of several hundred to several thousand $M_{\odot}$ could also be the explanation for the ultraluminous X-ray sources observed in external galaxies (Portegies Zwart et al. 2004; DiStefano et al. 2003), and could provide the missing link between the stellar-mass BHs formed as the end products of the stellar evolution of massive stars and the 10^6–$10^9\ M_{\odot}$ sized BHs found in galactic centers (Ebisuzaki et al. 2001).

Bahcall & Wolf (1976) showed that an equilibrium-flow solution for stars in the gravitational well around a BH exists and predicted that the stellar density will follow a power-law distribution $\rho = r^{-\alpha}$ with exponent $\alpha = 1.75$. While Peebles (1972) found a steeper slope, Monte Carlo simulations by Cohn & Kulsrud (1978) and Marchant & Shapiro (1980) confirmed the results of Bahcall & Wolf (1976). Because of the high stellar densities around the BH, tidal disruption of stars is important for the evolution of the system. Frank & Rees (1976) and Lightman & Shapiro (1977) found that stars on highly eccentric orbits dominate the consumption rate, since stars drift faster in angular momentum space than in energy space. Frank & Rees (1976) derived analytic formulae for the disruption rates that were later confirmed by Monte Carlo simulations (Marchant & Shapiro 1980; Duncan & Shapiro 1983). In the latter paper, the authors also showed that BHs in globular clusters preferentially disrupt those stars most tightly bound to the BH, while in galactic nuclei the disruption process should be dominated by stars not bound to the BH. The gas lost from disrupted stars is either accreted onto the central BHs or lost in a stellar wind because of radiation drag, with the first process dominating for high enough BH masses (David et al. 1987).

Stellar collisions could also be an important process, although for the low-mass BHs expected in globular clusters, Cohn & Kulsrud (1978) found that the collision rate of stars is ~30 times smaller than their consumption rate by the BH. Similarly, Murphy et al. (1991) performed multimass Fokker-Planck calculations and found that in low-density galactic nuclei stellar disruptions happen more often than stellar collisions.

Recently, Amaro-Seoane et al. (2004) followed the evolution of a system of equal-mass stars with a central BH by means of an anisotropic gaseous model and found a strong BH growth accompanied by the expansion of the cluster. An overall cluster expansion due to the inward drift and tidal disruption of stars was also predicted by Shapiro (1977).

Although various aspects of the dynamical evolution of BHs in dense stellar systems have been studied in the literature, nobody has tried a self-consistent direct N-body simulation of

[1] Astrophysical Computing Center, RIKEN, 2-1 Hirosawa, Wako-shi, Saitama 351-0198, Japan.
[2] Department of Astronomy, University of Tokyo, 7-3-1 Hongo, Bunkyo-ku, Tokyo 113-0033, Japan.

the growth of the central BH. Moreover, simulations with approximate methods such as Monte Carlo or Fokker-Planck methods have been applied only to idealized systems. For example, with the exception of Bahcall & Wolf (1977) and Freitag & Benz (2002), most simulations so far considered only single-mass systems and ignored stellar evolution. Thus, although such studies are useful to gain a physical understanding of the problem, they do not tell us much about the actual behavior of star clusters with central BHs. Can an IMBH grow from a lower mass seed BH by accreting nearby stars? What will star clusters with an IMBH look like? Do they have cusps in surface luminosity? In the present and companion papers, we address these issues. Our focus will be mainly on the dynamics of star clusters containing BHs. This is because direct N-body simulations cannot be done for systems containing more than a few $\times 10^5$ stars. In addition, simplifying assumptions such as a fixed BH at the cluster center are most likely violated for stellar systems containing BHs of only a few hundred to a few thousand times the mass of a star.

2. DESCRIPTION OF THE RUNS

We simulated the evolution of star clusters containing between $N = 5000$ and 178,800 stars using the collisional Aarseth N-body code NBODY4 (Aarseth 1999) on the GRAPE6 boards of Tokyo University (Makino et al. 2003). All clusters were treated as isolated and followed King profiles initially. At the start of the calculation, the massive BHs were at rest at the cluster centers. We set up the initial models so that the systems were in dynamical equilibrium and the density profiles were the same as the corresponding King models without the central BHs. To achieve this, we calculated the new distribution function from the King model density profile and the potential obtained by the original King potential plus the BH potential, and generated positions and velocities of the stars using this new distribution function. Note that it is impossible to setup an equilibrium model with isotropic velocity dispersion, which has a flat core with finite central density around a BH (Tremaine et al. 1994; Nakano & Makino 1999). Thus, our initial model is not in exact dynamical equilibrium, and the 0.5% mass shell shows contraction of ~10% in case of a 5% BH mass. The effect is, however, much smaller than the initial contraction of the cluster with a central BH in Figure 5, which is caused by the development of an $\alpha = -1.75$ cusp because of thermal evolution and can therefore be neglected.

Two series of simulations were produced. In the first series, we followed the evolution of equal-mass star clusters with central BHs. These simulations were designed to identify the relevant physical mechanisms and compare our results with theoretical estimates and results reported in the literature. In the second series of simulations, we studied the dynamics of BHs in galactic globular clusters. We simulated multimass clusters containing $16,384 < N < 131,072$ stars and a central BH of $M_{\rm BH} = 1000\ M_\odot$. The results of these runs will be reported in a companion paper (Baumgardt et al. 2004).

In the present paper, stars were assumed to be tidally disrupted if their distance to the central BH was smaller than a fixed disruption distance that was either $r_t = 10^{-7}$, 10^{-8}, or 10^{-9} in N-body units. For solar-type stars, the radius against tidal disruption by a $1000\ M_\odot$ IMBH is 2.3×10^{-7} pc (Kochanek 1992, eq. [3.2]). Since the half-mass radius of a star cluster is of the order of 1 in N-body units and globular clusters have half-mass radii of several pc, the adopted tidal radii correspond approximately to the tidal radius of an $m = 1\ M_\odot$ main-sequence star in a globular cluster. We assumed that a star was immediately disrupted if it entered the region with $r < r_t$ and was unaffected outside this area. The mass of a tidally disrupted star was added to the mass of the central BH. To extrapolate the simulation results to larger N and to compare with other results, we always use fitting formulae that explicitly contain r_t and scale them appropriately.

So far our runs do not incorporate the effect of gravitational radiation, which should be unimportant for the dynamical evolution of a star cluster as long as the stellar density around the BH and its growth are dominated by main-sequence stars.

In this paper, all clusters start from an initial density profile given by a King model with $W_0 = 10.0$ and are composed of equal-mass stars. Table 1 summarizes other parameters. It first shows a number identifying the run and the number of cluster stars N. Shown next are the initial and final mass of the BH divided by the mass of a single star, the tidal radius of the BH, and the duration of the simulation. The latter two quantities are given in N-body units in which the constants of gravitation, total cluster mass, and total energy are given by $G = 1, M_{\rm Cl} = 1,$ and $E = -0.25$, respectively (Heggie & Mathieu 1986). The final columns contain a dimensionless constant describing the tidal disruption rate of stars and the total number of tidal disruptions. We organized the runs into four groups. In the first set we varied the BH mass and kept all other parameters constant. The next two groups contain runs where the number of cluster stars and the tidal radius was varied. The final group contains a few additional runs used in the paper.

3. THEORY

Stars in the innermost cusp around the BH, where the gravitational influence of the BH is dominating, move on essentially Keplerian orbits, with slight perturbations when they encounter other cluster stars. Bahcall & Wolf (1976) assumed that stars in the sphere of influence of the BH follow an isotropic distribution in velocity space and are absorbed if their energy becomes equal to the potential energy at the tidal radius. They then showed by Fokker-Planck calculations that the stellar density distribution follows a power law $\rho(r) \sim r^{-\alpha}$ with $\alpha = 7/4$ inside the sphere of influence of the BH down to the radius where the tidal disruption of stars becomes important. The cusp profile will extend out to a radius where the self-gravity of the stellar system cannot be neglected any more. If the BH mass is much smaller than the mass of the stars in the core, this happens when the velocity dispersion in the cluster core becomes comparable to the circular velocity of stars in the field of the BH:

$$r_i = \frac{GM_{\rm BH}}{\gamma \langle v_c^2 \rangle}. \tag{1}$$

We found that $\gamma = 2$ gives a good fit to the results of our simulations. The velocity dispersion of stars in the cluster core $\langle v_c^2 \rangle$ can be expressed in terms of the core density and radius as

$$\langle v_c^2 \rangle = \frac{4\pi G m n_c r_c^3}{3 r_c} = \frac{4\pi}{3} G m n_c r_c^2. \tag{2}$$

Hence, the influence radius is given by

$$r_i = \frac{3M_{\rm BH}}{8\pi m n_c r_c^2} \approx 15 r_c \frac{M_{\rm BH}}{m N_{\rm Cl}}, \tag{3}$$

where $N_{\rm Cl}$ is the number of cluster stars and we assume that the core contains roughly 3% of all stars in the cluster. Assuming that the cusp profile goes over into a constant density core with

TABLE 1
DETAILS OF THE PERFORMED *N*-BODY RUNS

Run Number (1)	N (2)	$M_{\rm BH}$ Initial / M_* (3)	$M_{\rm BH}$ Final / M_* (4)	r_t (5)	$T_{\rm end}$ (6)	k_D (7)	$N_{\rm Disruptions}$ (8)
1	80,000	266.0	827.0	10^{-7}	3000	72.0	561
2	80,000	800.0	1388.0	10^{-7}	2000	63.0	588
3	80,000	2660.0	3285.0	10^{-7}	2000	63.1	625
4	80,000	8000.0	8749.0	10^{-7}	2000	57.0	749
5	5,000	800.0	815.0	10^{-8}	2000	44.1	15
6	10,000	800.0	823.0	10^{-8}	2000	54.2	23
7	20,000	800.0	869.0	10^{-8}	2000	65.0	69
8	80,000	800.0	997.0	10^{-8}	2000	55.3	197
9	80,000	800.0	1388.0	10^{-7}	2000	63.0	588
10	80,000	800.0	997.0	10^{-8}	2000	55.3	197
11	80,000	800.0	851.0	10^{-9}	2000	73.2	51
12	16,000	2589.0	2735.0	10^{-7}	2000	75.6	146
13	20,000	200.0	338.0	10^{-7}	3000	53.9	138
14	35,700	1438.0	1705.0	10^{-7}	2000	63.0	267
15	65,536	3276.0	3513.0	10^{-8}	3000	76.9	237
16	178,800	461.0	1368.0	10^{-7}	2000	58.2	907

NOTE.—Col. (1): Number identifying the run. Col. (2): Number of cluster stars. Cols. (3) and (4): Initial and final mass of the BH divided by the mass of a single star. Col. (5): Tidal radius of the BH. Col. (6): Duration of the simulation. Col. (7): Dimensionless constant describing the tidal disruption rate of stars. Col. (8): Number of tidal disruptions. Cols. (7) and (8) are given in *N*-body units.

density n_c at r_i, the number of stars in the cusp can be estimated to be

$$N_{\rm cusp} = 4\pi \int_0^{r_i} n_c \left(\frac{r_i}{r}\right)^{1.75} r^2 dr = 250 \frac{M_{\rm BH}^3}{M_{\rm Cl}^3} N_{\rm Cl}, \quad (4)$$

which serves to give an order-of-magnitude estimate. For central BHs containing less than 1% of the total cluster mass, the central cusp itself contains only on the order of 10% of the BH mass in stars. Typical globular clusters would have BHs with masses of the order of 1000 $M_\odot$ if they follow the relation found by Ferrarese & Merritt (2000) and Gebhardt et al. (2000) for galaxies, making the detection of the central cusp in their density profile difficult even with the *Hubble Space Telescope* (Drukier & Bailyn 2003). In clusters in which the BH is more massive than the cluster core, an upper limit for r_i derives from the condition that the mass in stars inside r_i should be smaller than the mass of the central BH, i.e., $M(<r_i) \leq M_{\rm BH}$.

Frank & Rees (1976) found that $r_{\rm crit}$, the radius at which tidal disruption of stars becomes important, is significantly larger than the tidal radius, since relaxation lets stars drift faster in angular momentum space than in energy space. In order to account for this, they introduced the loss cone, which is the area in angular momentum space containing all orbits with minimum distances smaller than the tidal radius r_t of the BH. At a given radius r, the opening angle of the loss cone is given by

$$\theta_{\rm lc}^2 = \frac{2r_t}{3r} \quad (5)$$

for radii $r < r_i$. They then showed that the critical radius $r_{\rm crit}$ is approximately given by the radius where the time for stars to drift through the loss cone because of relaxation becomes longer than the crossing time. Inside $r_{\rm crit}$ stars cannot drift in and out of the loss cone before falling into the BH, so the loss cone is empty. Cohn & Kulsrud (1978) and Marchant & Shapiro (1980) performed two-dimensional Monte Carlo calculations of the evolution of a star cluster with a central BH that confirmed the loss cone concept. They determined disruption rates of stars and showed that tidal disruption of stars flattens the density profile inside $r_{\rm crit}$ but has little influence outside this radius.

Another process that can in principle be important is the wandering of the BH. A BH in a stellar system is forced to move because of three processes: stars bound to the BH force it to move around the common center of gravity, stars escaping from the core cause a recoil motion of the BH and the stellar core surrounding it, and passing unbound stars cause a Brownian motion of the BH in the center of the cluster. Lin & Tremaine (1980) investigated the role of the different processes and concluded that passing unbound stars have the largest effect on the BH. For a BH in a constant density core, they estimated the wandering radius to be given by

$$r_{\rm wand} = 0.9 r_c \sqrt{\frac{m}{M_{\rm BH}}}. \quad (6)$$

The wandering radius is difficult to determine in our simulations, since it hardly exceeds the distance of the innermost stars from the BH and is therefore within the statistical uncertainty with which the position of the density center can be determined. In addition, the innermost stars are so tightly bound to the BH that they follow the motion of the BH due to passing unbound stars as long as the unbound stars pass at large enough distances. This further complicates the determination of the density center. Chatterjee et al. (2002) gave a detailed discussion of BH wandering and performed *N*-body simulations that confirmed the validity of equation (6). The wandering of the BH will limit the formation of an $\alpha = 1.75$ cusp to models with high enough BH masses. It could also effect the capture rate of stars since the area of the loss cone is increased.

4. RESULTS

4.1. *Central Density Profile*

In order to determine the central density profiles, we have overlaid five snapshots from the time the simulation was

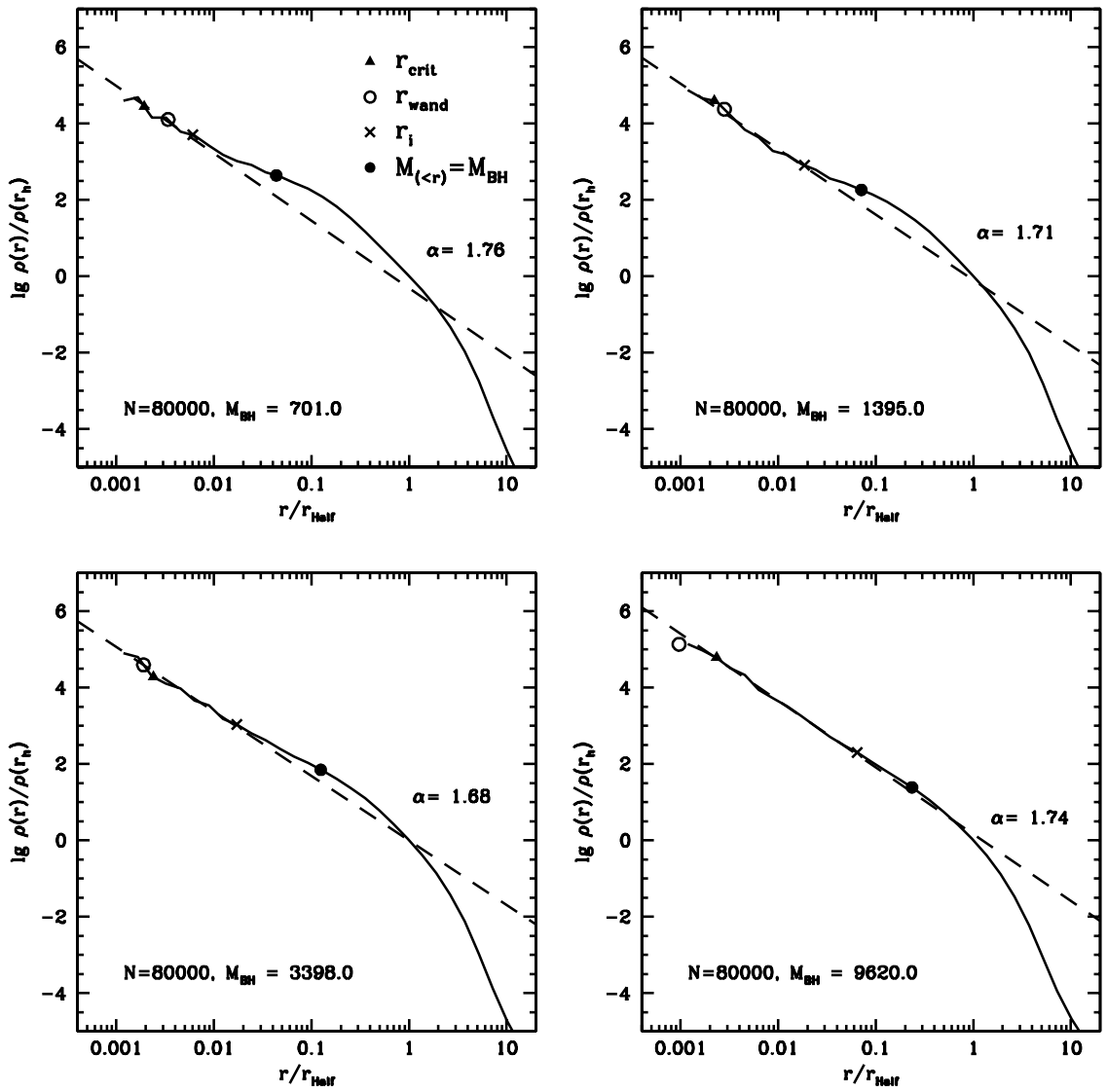

FIG. 1.—Density profiles at $T = 2000$ N-body units for clusters 1–4 from Table 1, which contain $N = 80,000$ stars and BHs of varying masses. Solid circles mark the radii where the mass in stars becomes comparable to the mass of the central BH, crosses mark r_i from eq. (1), open circles show $r_{\rm wand}$, and triangles show $r_{\rm crit}$. An $\alpha = 1.75$ power-law cusp forms inside r_i in all models. For the model with the most massive BH, the central cusp extends almost up to the radius where $M_{(<r)} = M_{\rm BH}$.

stopped for each cluster. All snapshots were centered on the BHs. Figure 1 depicts the final density profiles inside the half-mass radius for runs 1–4, which contain $N = 80,000$ stars and BHs with masses of $300 < M_{\rm BH}/m < 8000$. The influence radii defined by equation (1) are marked by crosses. Also shown are the radii where the mass in stars becomes comparable to the mass of the central BH (*filled circle*) and the wandering radii of the BHs (*open circle*). For all cases studied, the critical radii are significantly smaller than the influence radii r_i and of the same order as the distance of the innermost stars from the BH, so we cannot test the density profile inside $r_{\rm crit}$. The lack of stars inside $r_{\rm crit}$ points to an efficient destruction at radii $r < r_{\rm crit}$.

For the BH of a few hundred solar masses, an $\alpha = 1.75$ cusp cannot be found with certainty, since the number of stars inside r_i is too small. In addition, the wandering radius of the BH is almost as large as r_i, so the BH wandering will also flatten the profile. Clusters with more massive BHs show a clear $\alpha = 1.75$ cusp, in good agreement with the prediction from Fokker-Planck and Monte Carlo models. The cusps extend up to radii $r = r_i$ in all cases. As expected, r_i is significantly smaller than the radius where the mass in stars becomes comparable to the mass of the central BH unless the BH contains several percent of the cluster mass. If the BH contains more than ~5% of the total cluster mass, the $\alpha = 1.75$ cusp goes all the way up to the radius where the mass in stars becomes equal to the mass of the central BH.

Figure 2 depicts the central density profile for a number of small-N runs. The overall behavior is very similar to the high-N runs, showing that our results do not depend on the particle number. Extending our results to larger systems, we predict that in globular clusters only on the order of 50 to 100 stars follow the central cusp profile if the mass of the BH is $M_{\rm BH} = 1000\ M_\odot$. Since only a fraction of them will be bright enough to be easily detectable, it will be difficult to find the central cusp in the luminosity profile of the cluster. In galactic nuclei with BH masses in the range $10^6\ M_\odot < M_{\rm BH} < 10^9\ M_\odot$, on the other hand, a considerable number of stars is in the $\alpha = 1.75$ cusp, so the detection of the BH through observation of the central density or velocity profile should in principle be possible.

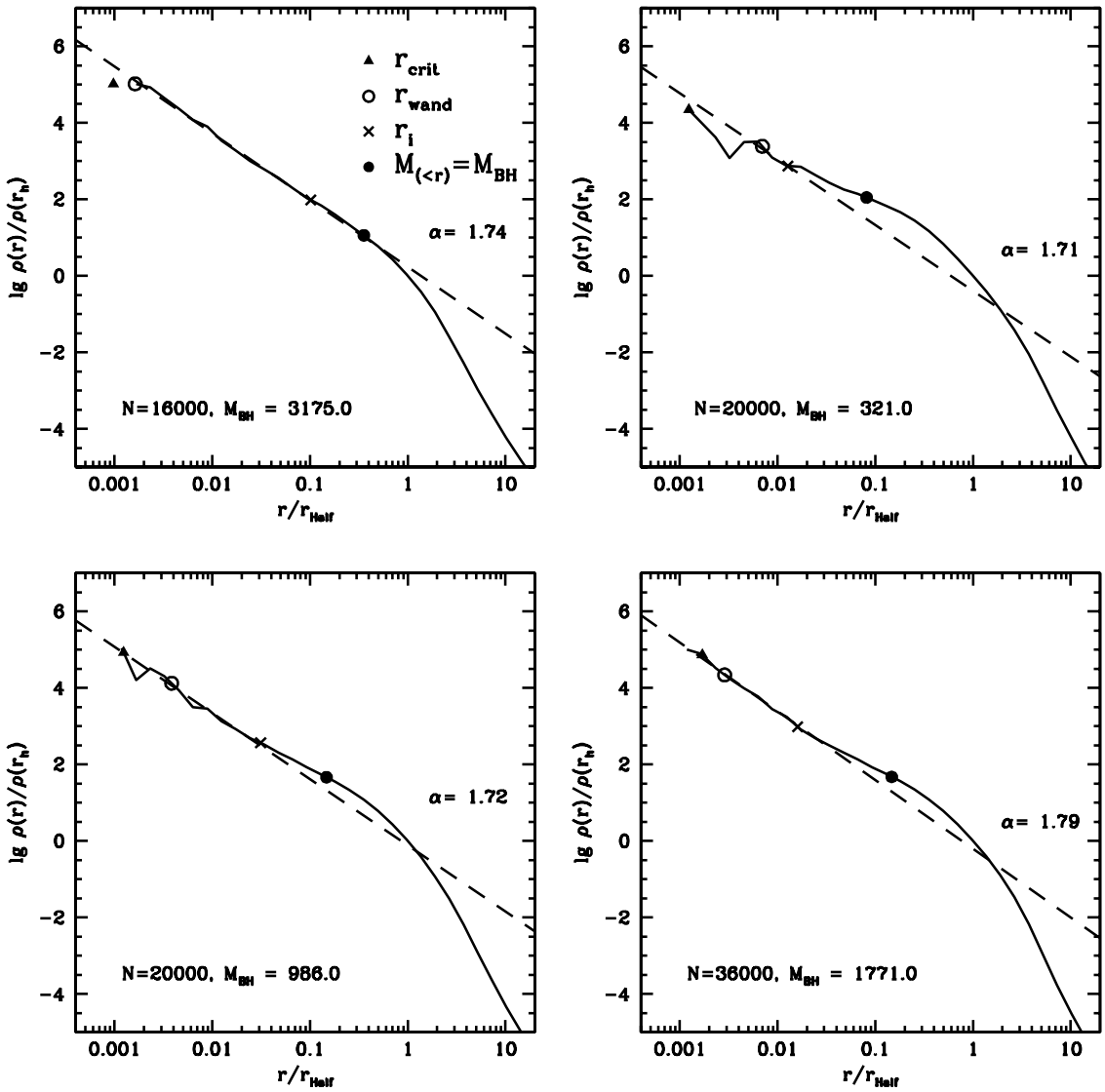

FIG. 2.—Same as Fig. 1, but for clusters of lower mass. All clusters have $\alpha = 1.75$ slopes inside the radii of influence of the BH r_i and flatter slopes outside this radius.

4.2. *Accretion Rates*

We can estimate the rate at which stars are disrupted by the central BH from the number of stars at radius $r_{\rm crit}$ and the size of the loss cone, divided by the crossing time at $r_{\rm crit}$:

$$D \sim \left| \frac{r^3 \theta_{\rm lc}^2 n(r)}{T_{\rm cr}} \right|_{r\,=\,r_{\rm crit}} .$$

Since in our simulations $r_{\rm crit}$ is much smaller than r_i, the density near the critical radius follows an $\alpha = 1.75$ power-law distribution:

$$n(r) = n_0 r^{-1.75}. \tag{7}$$

Following Frank & Rees (1976), the critical radius can be calculated to be

$$r_{\rm crit} = 0.2 \left(\frac{r_t M_{\rm BH}^2}{m^2 n_0} \right)^{4/9} . \tag{8}$$

Hence, we obtain for the disruption rate

$$D \sim \sqrt{G} \left| \frac{r_t M_{\rm BH}^{1/2}}{r^{5/4}} \right|_{r\,=\,r_{\rm crit}} = k_D \sqrt{G} \frac{r_t^{4/9} n_0^{14/9} m^{10/9}}{M_{\rm BH}^{11/18}} . \tag{9}$$

Figure 3 shows the evolution of the disruption rate as a function of time for clusters with a range of BH masses. In all runs the tidal disruption rates decrease because of the cluster expansion, which is discussed in the next paragraph. The cluster expansion decreases the stellar density near $r_{\rm crit}$ and increases the crossing time, thereby decreasing D. Solid lines show expected disruption rates according to equation (9), calculated by determining n_0 from the actual N-body data and the constants k_D from a best fit to the overall disruption rate. The time evolution of the disruption rates calculated this way agrees very well with the one found in the N-body

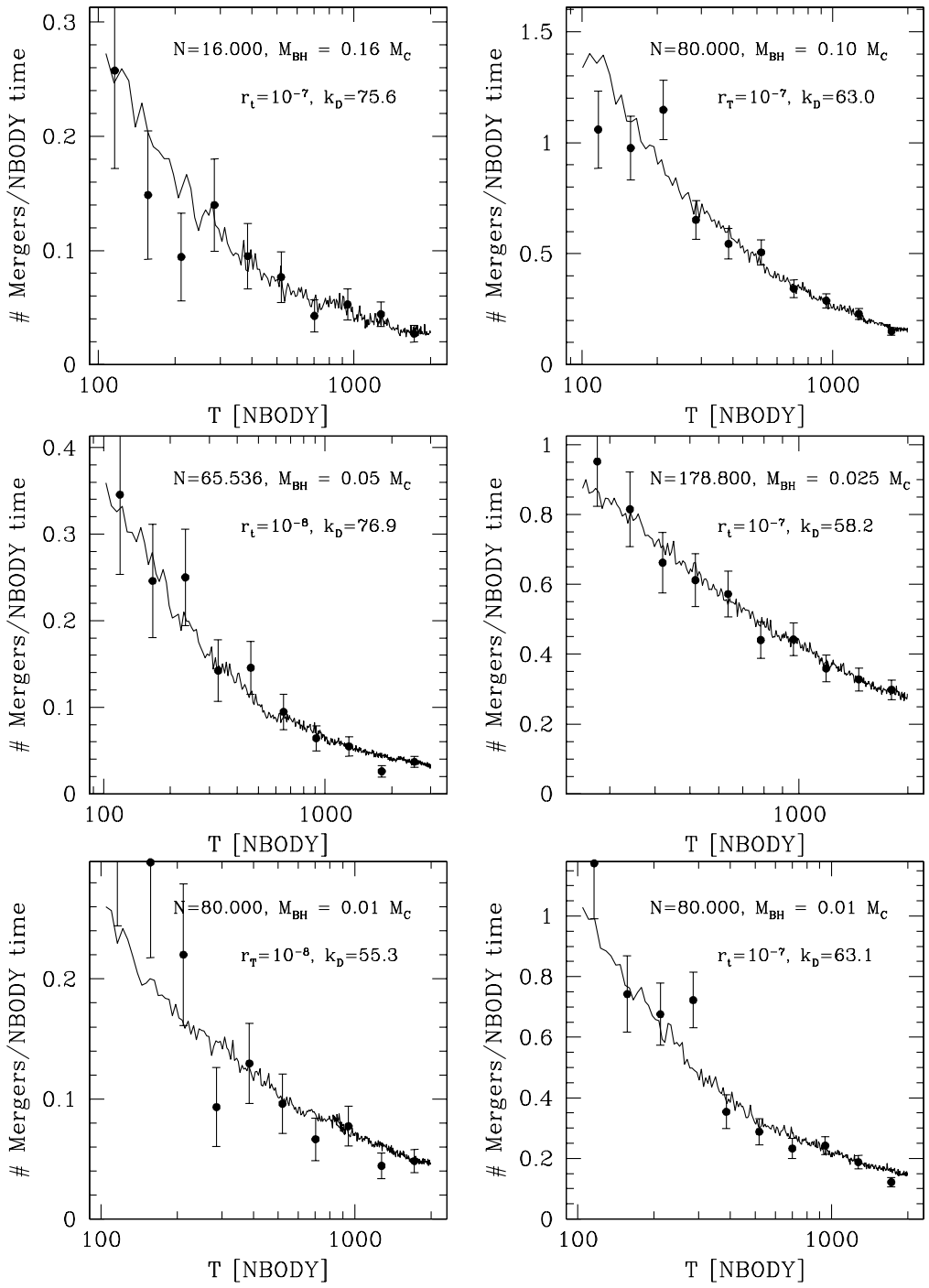

FIG. 3.—Evolution of the tidal disruption rate of stars with time for six different clusters. Points with error bars are results from *N*-body simulations. Solid lines show a fit according to eq. (9) with the constants k_D adjusted to match each case. The tidal disruption rate drops because of the expansion of the clusters. There is good agreement between the k_D values for the different clusters.

simulations. In addition, the constants k_D determined for the different simulations also agree reasonably well with each other and most are compatible with an average of $k_D = 65$ (see Table 1).

In order to calculate the collision rate in physical units, we assume that the tidal radius of a star with radius R_* and mass m is given by

$$r_t = 1.3\ R_* \left(\frac{M_{\rm BH}}{2m}\right)^{1/3} \tag{10}$$

(Kochanek 1992, eq. [3.2]). We then obtain for the tidal disruption rate

$$D = \frac{0.00588}{100\ \rm Myr}\left(\frac{R_*}{R_\odot}\right)^{4/9}\left(\frac{n_0}{\rm pc^{-1.25}}\right)^{14/9} \times \left(\frac{m}{M_\odot}\right)^{26/27}\left(\frac{M_{\rm BH}}{1000\ M_\odot}\right)^{-25/24}. \tag{11}$$

Although equation (11) seems to indicate that D decreases with the BH mass, this is not the case since the cusp density constant

n_0 also depends on the BH mass and the central density n_c. It is, however, interesting to apply equation (11) to cusps of observed systems. Genzel et al. (2003), for example, derived a stellar density of $\rho = 1.2 \times 10^6\ M_\odot\ \mathrm{pc}^{-3}$ at a distance of $r = 0.38$ pc from the galactic center. They found that the density inside this radius rises with a power law with power $\alpha = 1.4$, while it falls off with $\alpha = 2.0$ outside this radius. Both values are not too far from the $\alpha = 1.75$ slope in our runs. Using their density, we find $n_0 = 2.21 \times 10^5\ \mathrm{pc}^{-1.25}$ if we assume an average stellar mass of $\langle m \rangle = 1\ M_\odot$. From equations (8) and (11) we then obtain a critical radius of $r_{\mathrm{crit}} = 1.2$ pc and a total number of disruptions of $D = 30,000$ per $T = 100$ Myr for a central BH mass of $M_{\mathrm{BH}} = 3 \times 10^6\ M_\odot$. Tidal disruption of stars could therefore play an important role for the growth of the galactic center BH.

In order to apply equation (11) to systems with a constant density core, we assume that the cusp density goes over into a constant-density core with density n_c at $r = 2r_i$. With the help of equation (3), we then obtain

$$D = \frac{17504.9}{100\ \mathrm{Myr}} \left(\frac{R_*}{R_\odot}\right)^{4/9} \left(\frac{m}{M_\odot}\right)^{-95/54} \times \left(\frac{n_c}{\mathrm{pc}^{-3}}\right)^{-7/6} \left(\frac{r_c}{\mathrm{pc}}\right)^{-49/9} \left(\frac{M_{\mathrm{BH}}}{1000\ M_\odot}\right)^{61/27}. \quad (12)$$

The powers of the different factors are the same as those obtained by Frank & Rees (1976) for the case $r_{\mathrm{crit}} < r_i$ (eq. [16*a*] in their paper). Our disruption rate is about a factor of 2 larger than theirs. From equation (2), we can obtain an alternative expression that uses the core velocity dispersion, which is easier to observe than the core radius:

$$D = \frac{22.9}{100\ \mathrm{Myr}} \left(\frac{R_*}{R_\odot}\right)^{4/9} \left(\frac{m}{M_\odot}\right)^{26/27} \left(\frac{n_c}{5 \times 10^4\ \mathrm{pc}^{-3}}\right)^{14/9} \times \left(\frac{v_c}{10\ \mathrm{km\ s}^{-1}}\right)^{-49/9} \left(\frac{M_{\mathrm{BH}}}{1000\ M_\odot}\right)^{61/27}. \quad (13)$$

This formula agrees with the one from Cohn & Kulsrud (1978, eq. [66]), who obtained nearly the same dependence of the disruption rate on the different physical parameters. Our disruption rate is smaller by ~33%, which indicates a very good agreement given the errors involved by assuming that the central cusp goes over directly into a constant density core, which is a significant simplification of the real situation (Figs. 1 and 2).

Typical parameters for the densest globular clusters are $n_c = 5 \times 10^5\ \mathrm{pc}^{-3}$ and $v_c = 15\ \mathrm{km\ s}^{-1}$. While a $M_{\mathrm{BH}} = 1000$ BH should be able to double its mass within a few Gyr from disrupted main-sequence stars in such a cluster, it does not seem possible to grow a 1000 $M_\odot$ BH from a 100 $M_\odot$ progenitor within a Hubble time. A more detailed discussion must, however, also take the mass distribution of the stars into account, which will be the focus of a follow up paper.

Figure 4 shows the eccentricity distribution of stars that are tidally disrupted by the BH and their semimajor axis a in relation to the critical radius. Stars that are disrupted by the central BH move on very eccentric orbits on average, with practically all of them having orbital eccentricities $e > 0.999$ on the final orbit prior to disruption, in good agreement with the idea that the drift in angular momentum space is more important than the drift in energy space for the feeding of the BH. The lower panel shows the semimajor axis distribution.

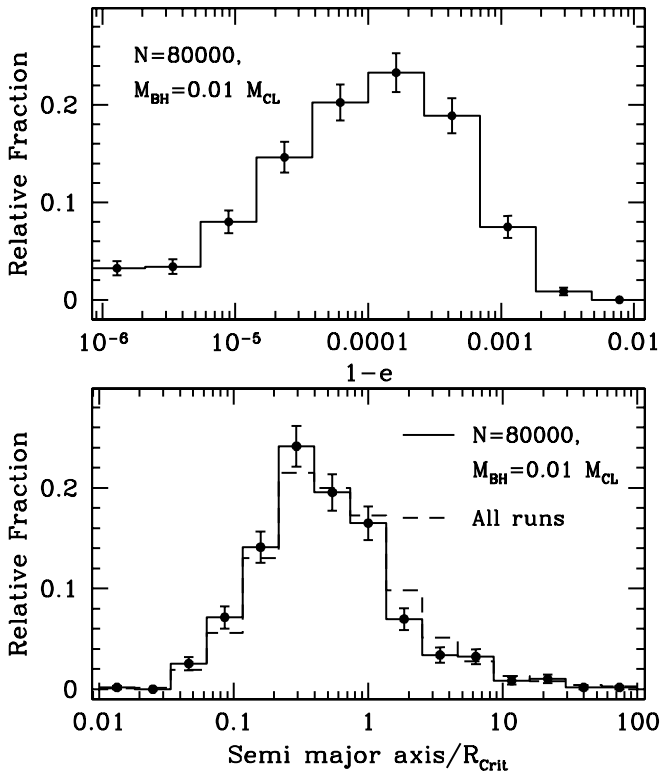

FIG. 4.—Distribution of orbital eccentricities (*top*) and semimajor axis (*bottom*) of stars being tidally disrupted by the central BH for run 2, which has $N = 80,000$ and $M_{\mathrm{BH}} = 0.01\ M_{\mathrm{Cl}}$. All disrupted stars move on highly eccentric orbits, implying that drift in angular momentum space is the main process contributing to the tidal disruption of stars. Stars being tidally disrupted by the BH originate from approximately the critical radius (*bottom*).

Most stars disrupted by the BH have semimajor axis $a \leq r_{\mathrm{crit}}$. The median a turns out to be about $a = 0.5 r_{\mathrm{crit}}$. Since the eccentricity is nearly unity, the apobothron distance, i.e., the maximum BH distance on the last orbit before disruption, is $r_a = 2a$, so $r_a \approx r_{\mathrm{crit}}$, in good agreement with our numerical estimates for r_{crit}. We do not find strong evidence for significant differences in the distribution of a/r_{crit} in the different runs, so we can average them. The dashed curve in the lower panel shows the distribution averaged over all runs, which is nearly identical to the solid curve for one particular run. Since in our runs $r_{\mathrm{crit}} \ll r_i$, all stars being disrupted by the BH are tightly bound to it. As these stars are constantly replenished by less bound stars from outside r_i, energy conservation requires that the rest of the system gains energy and expands. This expansion will be the focus of the next section.

4.3. *Cluster Evolution*

The evolution of Lagrangian radii of two clusters is depicted in Figure 5. Shown is cluster 15, which contains $N = 65,536$ stars and a BH of $M_{\mathrm{BH}} = 0.05\ M_{\mathrm{Cl}}$ and a second cluster with the same initial density profile and number of cluster stars but no massive BH. The cluster without the BH goes into core collapse at $T = 1460.0$ N-body units. Core collapse is halted when binaries form in the core and interactions between the binaries and passing cluster stars heat the cluster and lead to an overall expansion of the cluster. Since the cluster is isolated and we did not allow for stellar collisions, no characteristic length scale exists and the expansion is proportional to

$$r \sim t^{2/3} \quad (14)$$

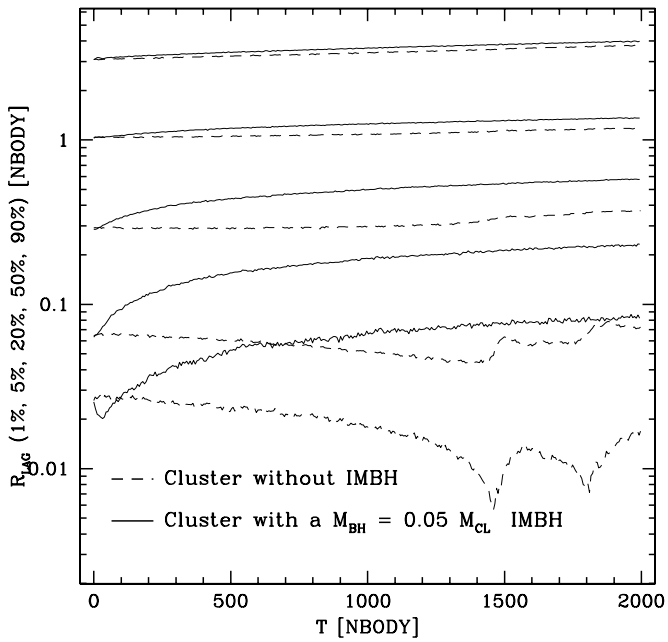

FIG. 5.—Evolution of Lagrangian radii for two $N = 65,536$ star clusters, one with a massive BH and one without. The cluster without a BH goes into core collapse at $T = 1450$ N-body units and expands during the postcollapse phase because of energy generated by binaries formed in the core. The cluster with a BH expands from the start since energy exchanges between stars in the cusp around the BH provide the energy for the expansion.

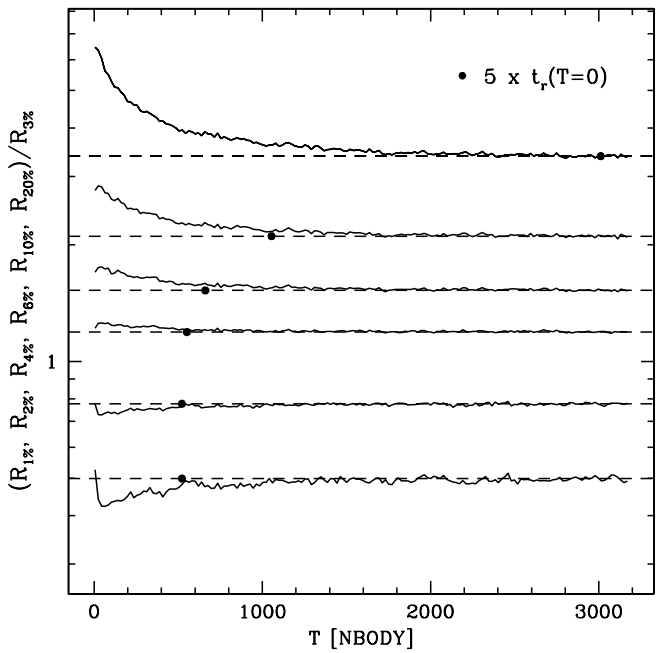

FIG. 6.—Ratio of the Lagrangian radii to the 3% Lagrangian radius for the run with a 1000 $M_\odot$ BH from Fig. 5 (*solid lines*). Dashed lines show average ratio near the end of the simulation. After an initial phase in which the core is readjusting itself, the ratios of different radii become constant and the cluster expansion becomes self-similar. The black dots show the time when five initial relaxation times have passed at the different radii.

in the postcollapse phase (Giersz & Heggie 1994; Baumgardt et al. 2002). The cluster core undergoes gravothermal oscillations, since the number of active binaries in the core is small: a look at the cluster data shows that most of the time there is only one binary in the core that powers the expansion, in agreement with theoretical expectations (Goodman 1984). If this binary is expelled, the cluster center recollapses again and forms new binaries. In contrast, the cluster with a central BH expands right from the start and without core oscillations, since the expansion is powered by energy exchanges of stars in the central cusp around the BH, which remains in the cluster core because of its high mass. Only the innermost radii show a short collapse phase in the beginning, when the central cusp profile is created. Binaries cannot be responsible for the heating since their formation is suppressed by the high stellar velocities in the cusp and the strong gravitational field of the BH, which disrupts binaries. Consequently, no stable systems formed in our runs. Figure 5 confirms that a central BH can act as a heat source similar to the effect of binaries in postcollapse clusters.

Figure 6 shows the evolution of Lagrangian radii for cluster 15, which has $N = 65,536$ stars and a BH mass of 0.05 $M_{\rm Cl}$. All radii are divided by the 3% Lagrangian radius. If we calculate the local relaxation time at different Lagrangian radii from Spitzer (1987),

$$t_r = 0.065 \frac{v_m^3}{nm^2 \ln \Lambda}, \qquad (15)$$

with $\Lambda = 0.11N$ (Giersz & Heggie 1994), it can be seen that the ratio of the different radii to the 3% radius becomes constant after about five local relaxation times have passed. The expansion of the cluster therefore becomes self-similar beyond this time. Since the relaxation time increases with radius, the equilibrium profile is established first for radii nearest to the BH and then forms at larger radii. We obtain similar results for the other clusters. Most globular clusters have central relaxation times much less than a Hubble time (Spitzer 1987, Fig. 1.3), so we expect that they have reached equilibrium profiles in their centers if they contain massive BHs.

Closely related to the expansion of a cluster is the escape of stars. The energy distribution of stars escaping from the two clusters of Figure 5 is depicted in Figure 7. We measure the energies of escaping stars after they have left the cluster and divide the energies by the average kinetic energy of all stars still bound to the cluster at the time the escape event happens. The energy distribution of escapers in the case of no BH shows two distinct maxima, corresponding to escapers created by a slow diffusion process in the outer parts of the cluster and escapers created by three-body encounters in the cluster core. We can fit the whole escaper distribution by the sum of two Gaussians with maxima at $\langle \log E/E_{\rm kin} \rangle = 0.1$ and 10.0, similar to what Baumgardt et al. (2002) found for isolated clusters with lower N.

Although the structure of both clusters is not exactly the same and a direct comparison is therefore difficult, it can be seen that the number of escapers is increased if a BH is present (note the different scale on the y-axis in the lower panel). At $T = 1450$, at which time the cluster without IMBH reached core collapse, the cluster with a BH has created ~6.5 times as many escapers as the cluster without BH. In the postcollapse phase, the number of escapers per time is approximately equal in the two runs. Since the process for generating escapers is different, the energy distribution of escapers in the two runs is also different, especially at the high-E end. Escapers created by distant encounters outside the core should still be present in the BH case. If we subtract the distribution found for stars escaping because of distant encounters in case of no BH

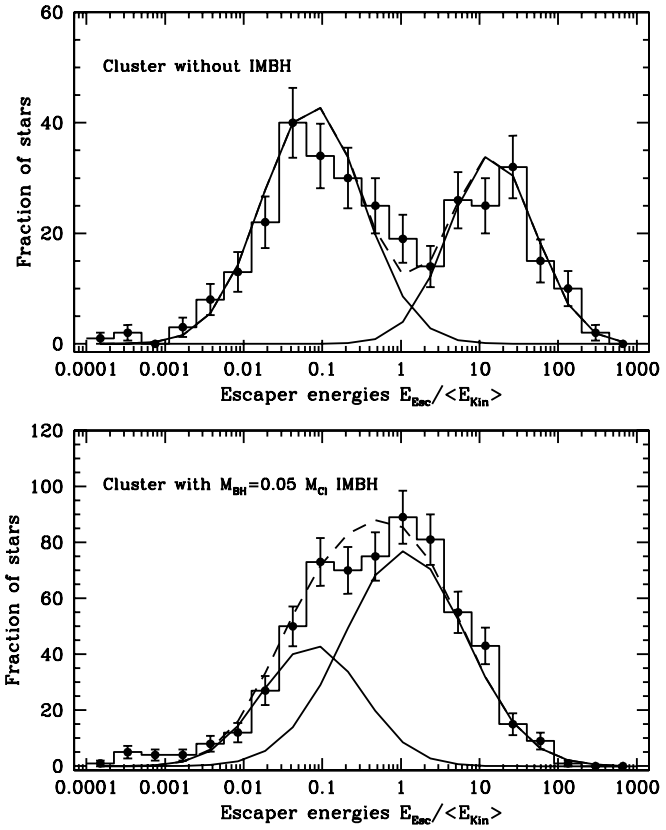

FIG. 7.—Distribution of escape energies for the clusters of Fig. 5. For a cluster without a central BH, two distinct peaks are visible, corresponding to stars escaping because of distant two-body encounters and close three-body encounters involving binaries. In the cluster with a BH, most stars escape because of close encounters in the cusp around the BH. Solid lines are Gaussian fits to the energy distributions of different escape mechanisms (see text). Dashed lines show the sums, which fit the *N*-body results very well.

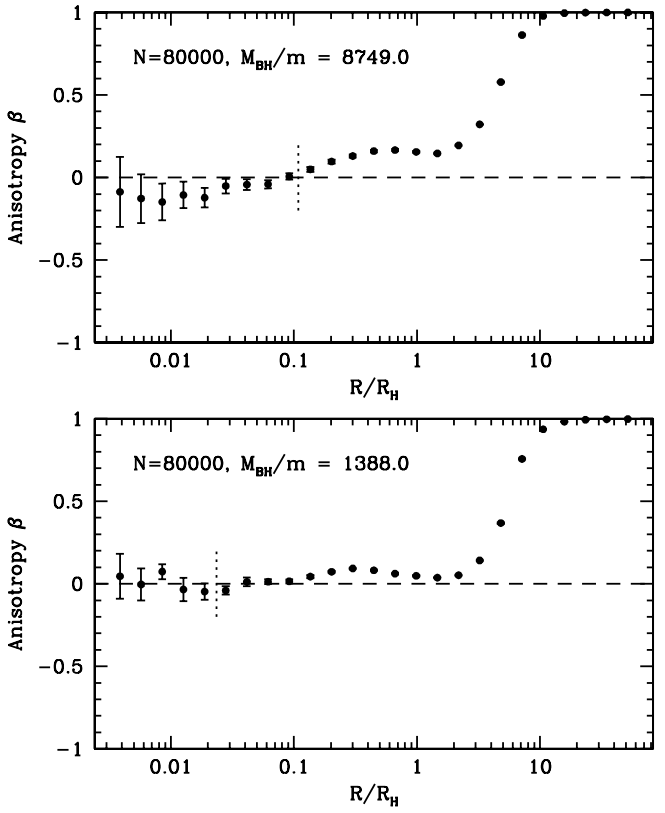

FIG. 8.—Anisotropy as a function of radius for two clusters with $N = 80,000$ stars. The dotted vertical line marks the radius of influence of the BH. The cluster with the larger BH has a slight tangential anisotropy in the center because of the preferential disruption of stars on radial orbits.

from the BH case, we can fit the remaining distribution by a Gaussian distribution with mean $\langle \log E/E_{\rm kin} \rangle = 1.0$. These are escapers created in the high-density cusp around the BH. From Figure 7 we can estimate that ~200 stars escape by distant encounters and ~420 by close encounters in the cusp. During the same time, 211 stars are disrupted by the BH, so stars in the cusp have a larger chance of escape than disruption. Nevertheless, the energy carried away by the escapers is small compared to the energy created by the tidal disruption of stars, since we find that ~10 times as much energy is created than is taken away by escapers. The energy created by the tidal disruption of stars therefore enters mostly the cluster expansion. We obtain this result in all simulated clusters.

Mathematically, when a star is accreted to the central BH the binding energy of the star cluster is reduced by an amount the same as the binding energy of the star and the IMBH. In other words, the cluster is heated up. Since almost all stars accreted to BHs are strongly bound to IMBHs, accretion almost always resulted in heating. From a physical point of view, accreted stars increased their binding energy by giving their kinetic energies to field stars, thus heating the cluster. How much heat the accreted star gave is simply determined by its binding energy at the moment of the accretion. The effective energy generation by the stars disrupted by the BH can be estimated from the disruption rate multiplied by the typical energy of a star disrupted by the BH. Since $r_{\rm crit} \gg r_t$, stars disrupted by the BH are on nearly radial orbits, so the energy of a star is equal to the potential energy at $r_{\rm crit}$: $E_* = GM_{\rm BH}m/r_{\rm crit}$. We therefore obtain

$$\dot{E} = D \times E_* = k_D G^{3/2} \frac{m^3 n_0^2}{M_{\rm BH}^{1/2}}. \tag{16}$$

Interestingly, there is no dependence of the energy generation rate on the tidal radius r_t. For low-mass BHs, most of the potential energy comes from the gravitational interaction between the stars themselves. The energy needed to expand the cluster is therefore given by

$$\dot{E} = k \frac{GM_{\rm Cl}^2}{r_h^2} \dot{r}_h, \tag{17}$$

with r_h being the cluster's half-mass radius and k a constant of the order of unity. Combining both equations and assuming that the cusp profile goes over into a constant density core at r_i, we obtain

$$\dot{r}_h \sqrt{r_h} = \sqrt{G} 30 k_D \left(\frac{r_h}{r_c}\right)^{2.5} \frac{M_{\rm BH}^3 m}{M_{\rm Cl}^{3.5}}. \tag{18}$$

With $k_D = 65$, $M_{\rm Cl} = 1.0$, and $r_h/r_c \approx 10$, this gives

$$r_h^{3/2} - r_{h0}^{3/2} = 6 \times 10^5 M_{\rm BH}^3 m t. \tag{19}$$

The time dependence is the same as in the self-similar case, $r \sim t^{2/3}$, since the energy generation rate is independent of the tidal radius, so no characteristic length scale exists.

Figure 8 depicts the velocity anisotropy profile for runs 2 and 4, which have $N = 80,000$ clusters and BHs containing 1% and 10% of the total cluster mass. The anisotropies were defined as

$$\beta = 1 - \frac{\sum_i v_t^2}{2\sum_i v_r^2}, \tag{20}$$

where v_r and v_t are the radial and tangential velocities of each star and the sum runs over all stars in a radial bin. No significant degree of anisotropy can be detected in the cluster with the small BH inside the influence radius of the BH. The cluster with the more massive BH has a slightly tangentially anisotropic velocity dispersion, similar to what Cohn & Kulsrud (1978) found in their Fokker-Planck calculations for stars inside the influence radius of the BH. The reason is the preferential disruption of stars on radial orbits and the fact that more stars are disrupted in a cluster with a more massive BH. Amaro-Seoane et al. (2004, their Fig. 8) obtained a radially anisotropic profile of $r_{\rm crit} < r < r_i$, which could be due to their very large half-mass radius at the end of the run, which decreases the merging rate of stars. In any case, the small amount of anisotropy together with the small number of stars inside $r = r_i$ makes an observation of this effect for globular clusters almost impossible, although it might be detectable in galactic nuclei. For isolated clusters, cluster halos are buildup from stars scattered out of the center that move on very radial orbits. Therefore, both clusters have radially anisotropic profiles outside the half-mass radius. For any realistic cluster, the tidal field would cause an isotropization of the stellar orbits.

5. CONCLUSIONS

We report the first results of self-consistent N-body simulations of star clusters composed of equal-mass stars and a central massive BH. We find that in clusters with a massive central BH a $\rho \propto r^{-1.75}$ power-law cusp forms inside the sphere of influence of the BH, in good agreement with predictions from Fokker-Planck and Monte Carlo simulations. In star clusters where the BH mass is less than a few percent of the total cluster mass, the cusp contains only a fraction of the BH mass in stars. The minimum BH mass needed to form an $\alpha = 1.75$ cusp is several 100 $M_\odot$ for a typical globular cluster. Otherwise, the cusp contains too few stars to be significant. For a BH mass less than a few percent of the total cluster mass, the density profile is shallower than $\alpha = 1.75$ outside the radius of influence r_i of the BH. For more massive BHs, the $\alpha = 1.75$ cusp extends all the way through the core.

The cusp profile forms from the inside out and it takes about five local relaxation times until it is established at a given radius. Since the central relaxation times of globular clusters are of the order of 10^7–10^8 yr, globular clusters should have $\alpha = 1.75$ power-law cusps in their centers and will evolve more or less along a sequence of equilibrium profiles if they contain massive BHs. Inside the radius of influence of the BH, the velocity profile is slightly tangentially anisotropic because of the tidal disruption of stars on radial orbits. Since the magnitude of this effect is small, it is unlikely that it will be detectable except for star clusters with very massive BHs.

Our simulations confirm the merging rates found in Fokker-Planck simulations and from analytic estimates. Tidal disruption of stars could play an important role for the current growth of the supermassive BH at the Galactic center and the growth of intermediate-mass BHs in dense star clusters. However, the formation of an intermediate-mass BH out of a stellar mass BH in a globular cluster by tidal disruption of stars alone seems impossible. A massive BH in a star cluster merges mainly with tightly bound stars from its direct vicinity. These stars are constantly replaced by less bound cluster stars that drift inward because of relaxation. This causes an overall expansion of the cluster. BHs can therefore halt the core collapse of globular clusters, similar to the effect of binaries in postcollapse clusters. As in the case of an expansion driven by a central population of binaries, the expansion is self-similar, i.e., $r \sim t^{2/3}$.

We are grateful to Sverre Aarseth for his constant help with the NBODY4 code. We also thank the referee, Fred Rasio, for a careful reading of the manuscript and useful comments. H. B. is supported by the Japan Society for the Promotion of Science through Grant-in-Aid for JSPS fellows 13-01753.

REFERENCES

Aarseth, S. J. 1999, PASP, 111, 1333
Amaro-Seoane, P., Freitag, M., & Spurzem, R. 2004, MNRAS, 352, 655
Bahcall, J. N., & Wolf, R. A. 1976, ApJ, 209, 214
———. 1977, ApJ, 216, 883
Baumgardt, H., Hut, P., & Heggie, D. 2002, MNRAS, 336, 1069
Baumgardt, H., Hut, P., Makino, J., McMillan, S., & Portegies Zwart, S. 2003a, ApJ, 582, L21
Baumgardt, H., Makino, J., & Ebisuzaki, T. 2004, ApJ, 613, 1143
Baumgardt, H., Makino, J., Hut, P., McMillan, S., & Portegies Zwart, S. 2003b, ApJ, 589, L25
Chatterjee, P., Hernquist, L., & Loeb, A. 2002, ApJ, 572, 371
Cohn, H., & Kulsrud, R. M. 1978, ApJ, 226, 1087
David, L. P., Durisen, R. H., & Cohn, H. N. 1987, ApJ, 313, 556
DiStefano, R., Friedman, R., Kundu, A., & Kong, A. K. H. 2003, ApJ, submitted (astro-ph/0312391)
Drukier, G. A., & Bailyn, C. D. 2003, ApJ, 597, L125
Duncan, M. J., & Shapiro, S. L. 1983, ApJ, 268, 565
Ebisuzaki, T., et al. 2001, ApJ, 562, L19
Ferrarese, L., & Merritt, D. 2000, ApJ, 539, L9
Frank, J., & Rees, M. J. 1976, MNRAS, 176, 633
Freitag, M., & Benz, W. 2002, A&A, 394, 345
Gebhardt, K., Rich, R. M., & Ho, L. C. 2002, ApJ, 578, L41
Gebhardt, K., et al. 2000, ApJ, 539, L13
Genzel, K., et al. 2003, ApJ, 594, 812
Gerssen, J., van der Marel, R. P., Gebhardt, K., Guhathakurta, P., Peterson R. C., & Pryor, C. 2002, AJ, 124, 3270
———. 2003, AJ, 125, 376
Giersz, M., & Heggie, D. C. 1994, MNRAS, 270, 298
Goodman, J. 1984, ApJ, 280, 298
Heggie, D. C., & Mathieu, R. D. 1986, in The Use of Supercomputers in Stellar Dynamics, ed. P. Hut & S. McMillan (Berlin: Springer), 233
Kochanek, C. S. 1992, ApJ, 385, 604
Kormendy, J., & Gebhardt, K. 2001, in AIP Conf. Proc. 586, 20th Texas Symp. on Relavistic Astrophysics, ed. J. C. Wheeler & H. Martel (New York: AIP), 363
Lightman, A. P., & Shapiro, S. L. 1977, ApJ, 211, 244
Lin, D. N. C., & Tremaine, S. 1980, ApJ, 242, 789
Makino, J., Fukushige, T., Koga, M., & Namura, K. 2003, PASJ, 55, 1163
Marchant, A. B., & Shapiro, S. L. 1980, ApJ, 239, 685
Murphy, B. W., Cohn, H. N., & Durisen, R. H. 1991, ApJ, 370, 60
Nakano, T., & Makino, J. 1999, ApJ, 525, L77
Peebles, P. J. E. 1972, ApJ, 178, 371
Portegies Zwart, S. F., Baumgardt, H., Hut, P., Makino, J., & McMillan, S. L. W. 2004, Nature, 428, 724
Shapiro, S. L. 1977, ApJ, 217, 281
Spitzer, L., Jr. 1987, Dynamical Evolution of Globular Clusters (Princeton: Princeton Univ. Press)
Tremaine, S., et al. 1994, AJ, 107, 634